THE JOURNAL OF PHYSICAL CHEMISTRY B

Article

pubs.acs.org/JPCB

# Theoretical Study of the Formation of Mercury ($Hg^{2+}$) Complexes in Solution Using an Explicit Solvation Shell in Implicit Solvent Calculations

Akef T. Afaneh,[†] Georg Schreckenbach,*[,†] and Feiyue Wang[‡]

[†]Department of Chemistry and [‡]Centre for Earth Observation Science, Department of Environment and Geography, University of Manitoba, Winnipeg, MB Canada, R3T 2N2

Supporting Information

**ABSTRACT:** The structures and harmonic vibrational frequencies of water clusters $(H_2O)_n$, $n$ = 1−10, have been computed using the M06-L/, B3LYP/, and CAM-BLYP/cc-pVTZ levels of theories. On the basis of the literature and our results, we use three hexamer structures of the water molecules to calculate an estimated "experimental" average solvation free energy of $[Hg(H_2O)_6]^{2+}$. Aqueous formation constants (log $K$) for $Hg^{2+}$ complexes, $[Hg(L)_m(H_2O)_n]^{2-mq}$, L = $Cl^-$, $HO^-$, $HS^-$, and $S^{2-}$, are calculated using a combination of experimental (solvation free energies of ligands and $Hg^{2+}$) and calculated gas- and liquid-phase free energies. A combined approach has been used that involves attaching $n$ explicit water molecules to the $Hg^{2+}$ complexes such that the first coordination sphere is complete, then surrounding the resulting $(Hg^{2+}\text{-}L_m)\text{-}(OH_2)_n$ cluster by a dielectric continuum, and using suitable thermodynamic cycles. This procedure significantly improves the agreement between the calculated log $K$ values and experiment. Thus, for some neutral and anionic Hg(II) complexes, particularly Hg(II) metal ion surrounded with homo- or heteroatoms, augmenting implicit solvent calculations with sufficient explicit water molecules to complete the first coordination sphere is required—and adequate—to account for strong short-range hydrogen bonding interactions between the anion and the solvent. Calculated values for formation constants of $Hg^{2+}$ complexes with $S^{2-}$ and $SH^-$ are proposed. Experimental measurements of these log $K$ values have been lacking or controversial.

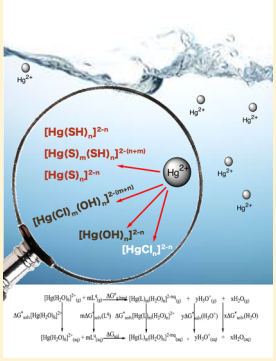


## 1. INTRODUCTION

Many chemical and biological reactions occur in water, where polar and ionic processes are much more favorable than in the gas phase. However, the aqueous solution cannot be represented by a single arrangement of solvent molecules but needs to be modeled by a very large number of such configurations. Although one way to overcome this problem is to model the solvent implicitly as a continuum[1−3] rather than with its detailed molecular structure, it is probable that the molecular nature of the solvent is often important, particularly in the immediate region of the solute. Accurate predictions of hydration free energies of cationic and anionic species, acid and base dissociation constants ($pK_a$ and $pK_b$), formation constants (log $K$), and oxidation−reduction potentials (ORP) are of critical importance in many areas of chemistry and biochemistry.[4−6] However, even with suitable thermodynamic cycles, continuum dielectric solvent models are inapt at predicting these thermodynamic values accurately, especially when dealing with ionic solutes that have high charge density with strong local solute−solvent interactions.[7−10] In addition, implicit solvation models fail for bare transition metal solvation. The models are not parametrized for these extreme cases. Usually, no reliable radii are available, and moreover, they do not take into account any of the various orbital interactions between the transition metal and its nearest neighbors.

One way to avoid these shortcomings of continuum solvent models is to take into account the first and possibly second solvation shells explicitly in the quantum mechanical calculations. This cluster is then embedded in a continuum solvation model.[11−37] Kelly et al. reported that the accuracy of the solvation free energies in aqueous media was improved by adding one explicit solvent molecule.[14,15] Pliego and Riveros indicated that a cluster-continuum solvent model with two to three water molecules gives better agreement with experiment for the calculation of the $pK_a$ of 17 organic molecules compared to those calculated using pure continuum solvent methods.[17,18] Solvation calculations for bare metal ions should at least contain a complete first coordination sphere of solvent (water) molecules.[19−28] Pliego and Riveros[18] showed that the hybrid cluster/continuum model is superior to the pure continuum methods, having root-mean-square errors of 2.2 $pK_a$ units as opposed to 7 $pK_a$ units for the SM5.42R and the polarizable continuum model (PCM)[38] methods for 17 small organic molecules. (The SM5.42R solvation model is based on charge model 2 and the generalized Born approximation for electrostatics augmented by terms that are proportional to the solvent accessible surface area of the solute.) Moreover, the ability of mixed implicit/explicit models to describe ion solvation has also been the subject of several investigations. Pratt and co-workers[19−21] were the first to use rigorous

**Received:** May 7, 2014
**Revised:** July 30, 2014
**Published:** July 30, 2014





dx.doi.org/10.1021/jp5045089 | J. Phys. Chem. B 2014, 118, 11271−11283

statistical thermodynamic considerations to combine hybrid solvation models with a monomer cycle. They found that the best estimates of the solvation free energies are obtained when the size of the solvent cluster ($n$) is selected variationally to produce the lowest solvation free energy. For ions with well-defined coordination numbers, the optimum $n$ is often equal to the number of solvent molecules in the first coordination shell. These authors also provided a detailed discussion of standard states pertinent to a monomer cycle.

In this paper, we are concerned with calculating the formation constants of $Hg^{2+}$ complexes,[35,39,40] $[Hg(L)_m(H_2O)_n]^{2-mq}$, where 2 and $-q$ are the charges of mercury and ligand L, respectively. Mercury is a globally distributed and toxic pollutant.[41,42] Large amounts of Hg have been released to the environment as a result of anthropogenic activities, resulting in an increase of global Hg flux by about a factor of 3 compared with the preindustrial natural Hg cycle.[41,43,44] Exposure of humans to Hg may cause damage to the central nervous system, heart, and immune system.[45]

Our interest in the formation constants of $[Hg(L)_m(H_2O)_n]^{2-mq}$ stems from a major uncertainty, over 12 orders of magnitude, associated with that of $HgS^0(aq)$ (mercury sulfide in aqueous media). Fitting their laboratory-based experimental data with the best-available thermodynamic constants, Benoit et al.[46−48] reported the neutral $HgS^0(aq)$ as the form of mercury to be accumulated by methylating bacteria in sulfidic sediment pore waters, forming methylmercury which is the primary mercury species for its neurological toxicity. However, this view of $HgS^0(aq)$ as the mercury species for methylation is contradicted by a field-based study.[49,50] It should be noted that the formation constant of $HgS^0(aq)$ has never been experimentally determined. The log $K$ value of −10 for $HgS^0(aq)$ used in Benoit et al.[46−48] was estimated by Dyrssen and Wedborg[51,52] based on linear free energy relationship (LFER) calculations with a correction term from the experimentally determined solubilities of CdS(s) and ZnS(s). The solubility product of CdS(s) used in Dyrssen and Wedborg[51,52] was subsequently found to be erroreous.[44] In fact, without the correction term, the LFER calculations would result in a log $K$ of −22.3 for HgS(0),[51,52] which would suggest that $HgS^0(aq)$ is not of quantitative importance at all in the Hg-sulfide system.

To better understand Hg speciation in sulfidic waters, we can construct thermodynamic cycles in several ways. The illustrations below show the simplest thermodynamic cycles to predict the solvation free energy of $[Hg(H_2O)_n]^{2+}$ in the presence of implicit and explicit solvent molecules. We modify some published methodologies for the computed solvation free energies to include standard state corrections for water molecules[14,15] or water clusters[29,33] present in the thermodynamic cycles. We use the same standard state for each species involved in the reaction under consideration.[53−55]

Explicit/implicit calculations of the solvation free energies of ions with different thermodynamic cycles (see Schemes 1 and 2 below) have been reported by several research groups.[17,21,29−33] However, the existing discrepancies among the calculated formation constants using different thermodynamic cycles and radii for $Hg^{2+}$ complexes have not been discussed in the literature. In this article, we compare the performance of two thermodynamic cycles in terms of how they predict the solvation free energy for $[Hg(H_2O)_n]^{2+}$. The results will then be applied to the prediction of the formation constants of $Hg^{2+}$ complexes with additional ligands other than water ($HO^-$, $Cl^-$, $HS^-$, and $S^{2-}$). On the basis of the present and literature results for explicit/implicit calculations, we provide a rationale for selecting the most appropriate thermodynamic cycle for the mixed explicit/implicit calculations of $Hg^{2+}$ complex formation constants.

**Scheme 1. Thermodynamic Cycle 1 (Monomer Cycle) for the Calculation of $\Delta G^*_{solv}([Hg(H_2O)_n]^{2+})$**

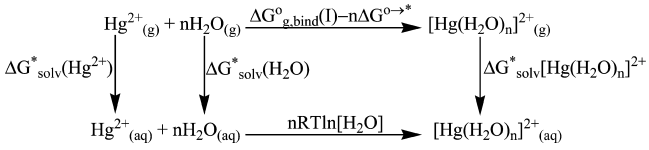


**Scheme 2. Thermodynamic Cycle 2 (Cluster Cycle) for the Calculation of $\Delta G^*_{solv}([Hg(H_2O)_n]^{2+})$**

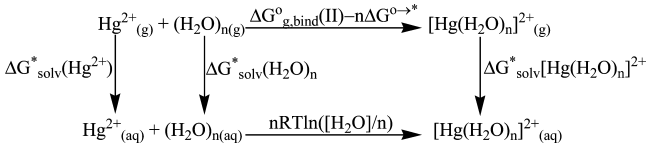


We calculate the solvation free energy and the formation constants of $Hg^{2+}$ complexes with $S^{2-}$ and $HS^-$ ligands on the basis of the following approach:

(1) We begin by studying water clusters for two purposes. First, they are used to test the accuracy of the level of theory by comparing the calculated dipole moment with the experimental values. Second, we use the water clusters in thermodynamic cycle 2 (see below) to calculate the solvation free energy of $[Hg(H_2O)_6]^{2+}$, $\Delta G^*_{solv}([Hg(H_2O)_6]^{2+})$.

(2) Six water molecules are coordinated to the Hg(II) metal ion in $[Hg(H_2O)_6]^{2+}$ to saturate the first shell of the Hg(II) ion.

(3) We use the $Cl^-$ and $HO^-$ ligands as further reference for our methodology. For monoligand complexes (one $Cl^-$ or $HO^-$), we need at least five water molecules to saturate the first shell, while we need four water molecules to saturate the first shell in the presence of two ligand substituents, and so on. These systems are used specifically to evaluate the effect of the atomic radii on the solvation free energy values of the water clusters and Hg(II) complexes. Six different types of radii are tested.

(4) Finally, the methods developed are applied to $HS^-$ and $S^{2-}$ species using thermodynamic cycles 1−4.

## 2. THERMODYNAMIC CYCLES FOR EXPLICIT/IMPLICIT MODELS

**2.1. Computation of $\Delta G^*_{solv}([Hg(H_2O)_6]^{2+})$.** We overcome the shortcomings of dielectric continuum models to accurately predict the formation constants of the $Hg^{2+}$ complexes by treating a part of the solvent explicitly. In this case, the solvation free energy of $[Hg(H_2O)_6]^{2+}$ can be calculated by using the thermodynamic cycles depicted in Scheme 1 or 2. For the monomer cycle (Scheme 1), the $Hg^{2+}$ ionic solute reacts with $n$ distinct water molecules. Conversely, a cluster of $n$ water molecules reacts with the ionic $Hg^{2+}$ solute in the cluster cycle (Scheme 2). In both cases, $\Delta G^\circ_{g,bind}$ is the free energy of complexation in the gas phase and $\Delta G^*_{solv}(X)$ is the standard


dx.doi.org/10.1021/jp5045089 | J. Phys. Chem. B 2014, 118, 11271−11283

solvation free energy for $X$ = $Hg^{2+}$, $H_2O$, $(H_2O)_6$, $[Hg(H_2O)_6]^{2+}$, and $[Hg(L)_m(H_2O)_n]^{2-mq}$.

The thermodynamic cycles should be corrected in the two layers (gas and aqueous layers) for both, reactants and products, to be in the same standard state. This is a key point of our discussion, and using the schemes presented here, this has been accounted for properly in the current approach. We evaluate all the thermodynamic quantities in Schemes 1−4 by using the 1 M ideal gas and the 1 M solutions as standard state.

The $\Delta G^*_{solv}(Hg(H_2O)_n)^{2+}$ from cycle 1 is given by[17]

$$\Delta G^*_{solv}([Hg(H_2O)_n]^{2+}) = \Delta G^*_{solv}(Hg^{2+}) - \Delta G^*_{g,bind}(I) - n\Delta G_{vap}(H_2O) \quad (1)$$

where $\Delta G^\circ_{solv}(Hg(II))$ is the solvation free energy of bare $Hg^{2+}$ which is taken directly from the output of the quantum-chemical program used, $\Delta G^*_{g,bind}$ is the gas-phase free energy of the complexation (upper leg of Scheme 1), and $\Delta G_{vap}(H_2O)$ is the vaporization free energy of water. It is defined by

$$\Delta G_{vap}(H_2O) = -\Delta G^*_{solv}(H_2O) - RT\ln[H_2O] - \Delta G^{\circ\to *} \quad (2)$$

where $\Delta G^*_{solv}(H_2O)$ is again taken directly from the program output. $RT\ln[H_2O]$ equals 2.38 kcal/mol. $\Delta G^{\circ\to *}$ is the free energy change of 1 mol of an ideal gas from 1 atm (24.46 L $mol^{-1}$) to 1 M at $T$ = 298.15 K and can be defined as[14,15]

$$\Delta G^{\circ\to *} = -T\Delta S^{\circ\to *} = RT\ln[V_0/V^*] = RT\ln(24.46) = 1.89\ \text{kcal/mol} \quad (3)$$

On the other hand, $\Delta G^*_{solv}([Hg(H_2O)_n]^{2+})$ from cycle 2 can be written as

$$\Delta G^*_{solv}([Hg(H_2O)_n]^{2+}) = \Delta G^*_{solv}(Hg^{2+}) - \Delta G^*_{g,bind}(II) + \Delta G^*_{solv}((H_2O)_n) + \Delta G^{\circ\to *} + RT\ln([H_2O]/n) \quad (4)$$

Here, $\Delta G^\circ_{solv}(Hg(II))$ and $\Delta G^*_{g,bind}$ are similar to the definitions of cycle 1 and $\Delta G^*_{solv}((H_2O)_n)$ is the solvation free energy of the water cluster.[37] It can be taken directly from the output of the quantum-chemical program or computed from Scheme 3.

**Scheme 3. Thermodynamic Cycle for the Formation of a Water Cluster**

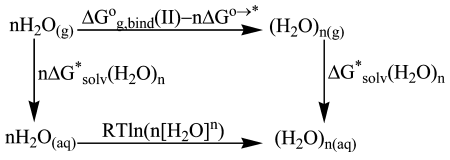


$\Delta G^{\circ\to *}$ and $RT\ln([H_2O]/n)$ are similar to cycle 1 except that in the second term the concentration is divided by the number of water molecules in the cluster. In applying eqs 1 and 4, the number of water molecules $n$ is taken as $n$ = 6. This amounts to a complete first solvation shell for the Hg(II) ion.

Note that eq 1 is exactly the equation that Pliego and Riveros[17] and Asthagiri et al.[20] derived by using a more formal description of the thermodynamics of solvation.

**2.2. Thermodynamic Cycle for the Formation of Water Clusters.** The change in the free energy that results from the rearrangement of the liquid water into the solvated water cluster, Scheme 3, is equal to zero.

$$nH_2O_{(l)55.34M} \rightarrow (H_2O)_{n(l)55.34/nM};\quad \Delta G^*_{aq,clust} = 0 \quad (5)$$

For the 1 M ideal gas and solution standard states, the concentration correction is given by

$$\Delta G^*_{aq,clust} = \Delta G^{l\to *}_{(H_2O)_n} - n\Delta G^{l\to *}_{H_2O} = nRT\ln[H_2O] - RT\ln([H_2O]/n) = RT\ln(n[H_2O]^{n-1}) \quad (6)$$

where $\Delta G^{l\to *}$ is the free energy change of $n$ moles of $H_2O$ gas from 55.34 M liquid to 1 M. Thus, the corrected solvation free energy of a water cluster (Scheme 3) is expressed as

$$\Delta G^*_{solv}((H_2O)_n) = \Delta G^\circ_{g,bind} + (n-1)\Delta G^{\circ\to *} + n\Delta G^*_{solv}(H_2O) + RT\ln(n[H_2O]^{n-1}) \quad (7)$$

**2.3. Thermodynamic Cycle for the Determination of log *K*.** Our methodology can be applied to any reaction in aqueous solutions. The explicit/implicit model has been applied to the calculation of the solvation free energies in Scheme 4. Thus, formation constants are calculated as

$$\log K = \frac{\Delta G^*_{g,bind} + \sum_P \Delta G^*_{solv} - \sum_R \Delta G^*_{solv}}{2.303RT} \quad (8)$$

where the two sums run over products (P) and reactants (R), respectively. $\Delta G^*_{g,bind}$ has been defined earlier (eq 1); it represents the binding free energies of the upper leg in the thermodynamics cycles in Schemes 1−4. The formation constant log $K$ (eq 8) is dependent on the solvation free energy of $[Hg(H_2O)_6]^{2+}$ that was calculated by using Scheme 1 or 2. Equation 8 can be used for the formation constant calculations of $[Hg(L)_m(H_2O)_n]^{2-mq}$ complexes. Equation 8 needs a correction term, which is necessary to correct the standard state of liquid water, which is 55.5 mol/L (log 55.5 = 1.74) by subtracting this value from eq 8 in the cases of $HO^-$ and $S^{2-}$. Bryantsev et al.[56] have recently highlighted that the incorrect assignment of the standard state for water molecules has resulted in systematic errors in a number of reports, and the issue was also addressed in an earlier report by Pliego.[17,18] The confusion is a result of the standard state for solutes in solution being 1 mol/L, and where water is acting as a coreactant, it is often (incorrectly) assumed to have a standard state of 1 mol/L as well.

## 3. COMPUTATIONAL METHODS

All structures were optimized at the B3LYP/cc-pVTZ/SDD level of theory[57−63] in the gas phase, unless otherwise noted. All stationary points were characterized by frequency calculations at the same level. Hybrid functionals and in particular the B3LYP method have been demonstrated to usually give accurate results for energies, structures, and vibrational properties of molecules and solids.[37,64,65] The gas phase calculations were followed with single points at the B3LYP/


dx.doi.org/10.1021/jp5045089 | J. Phys. Chem. B 2014, 118, 11271−11283

**Scheme 4. Thermodynamic Cycle for the Formation of $Hg^{2+}$ Complexes**

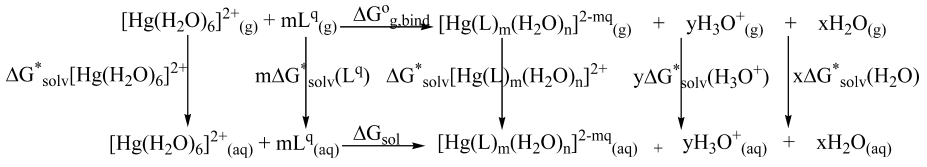


cc-pVTZ/SDD level in the aqueous environment. CPCM-SCRF[66] calculations at the B3LYP/cc-pVTZ//SDD(ECP) level were carried out on the stationary points to address solvation effects using the dielectric constant of water (78.39) in order to simulate the aqueous environment. The CPCM calculations were performed with tesserae of 0.2 Å$^2$ average size, the default value. These calculations were carried out with Gaussian 03 (G03).[67] Results reported in this article are those of G03-B3LYP-CPCM calculations, unless otherwise noted.

In implicit solvation models such as CPCM, the computed energies and properties of species depend on the cavity size. In this study, the united atom (UA) cavities (hydrogen atoms included with heavy atoms) UA0,[68] UAHF,[60,62] and UAKS,[60,62] as well as cavities having explicit hydrogens, UFF (radii from the UFF force field scaled by 1.1),[57,61,63] PAULING (Pauling atomic radii),[69] and BONDI (Bondi atomic radii),[70] were used to evaluate the aqueous solvation effects using CPCM. The UA0 cavity is built up using the united atom topological model (UATM) applied to atomic radii of the universal force field (UFF). By default, the UA0 model is chosen to build the cavity in G03. The UAHF and UAKS cavities use UATM with radii optimized for the HF/6-31G(d) and PBE0/6-31G(d) levels of theory, respectively. A set of radii from UFF is used for creating the UFF cavities. For the PAULING and BONDI cavities, each solute atom and group is assigned van der Waals values obtained from Pauling or Bondi atomic radii.

For test purposes, calculations have also been performed with the Northwest Computational Chemistry Package (NWChem), version 6.3.[71] We choose two levels of theories: First, the meta-GGA density functional, M06-L.[72] M06-L belongs to the M06 family, which has no HF exchange. Accordingly, M06-L is classified as a local functional. The other one is the long-range Coulomb attenuating method (CAM-B3LYP). CAM-B3LYP considers long-range interactions by comprising 19% of HF and 81% of B88 exchange at short range and 65% of HF plus 35% of B88 at long range.[73] The solvation energies were computed in these NWChem calculations using the conductor-like solvation model COSMO (with default parameters) of Klamt and Schüürmann.[74] Selected structures of Hg(II) complexes were reoptimized at the M06-L and CAM-B3LYP levels of theory.

The two functionals M06-L and B3LYP have also been augmented by the D3 dispersion corrections of Grimme and co-workers.[75] All DFT-D3 calculations were carried out using NWChem.[71]

In this study, three methods were evaluated for the calculation of the formation constants of the $Hg^{2+}$ complexes, log $K$ of eq 8: (i) the UAKS/CPCM and COSMO solvation free energies that were calculated directly and taken from the G03 and NWChem outputs, (ii) the monomer model of the water molecules using Scheme 1 and eq 1 to calculate the solvation free energy of $[Hg(H_2O)_6]^{2+}$, and (iii) the cluster models of the water molecules using Scheme 2 and eq 4 for the calculation of the solvation free energy for $[Hg(H_2O)_6]^{2+}$. In the case of the UAKS and monomer methods, the corresponding values of the water clusters were taken from the G03 output. For the cluster method, the solvation free energies of the water clusters were calculated using Scheme 3 and eq 7. Finally, Scheme 4 and eq 8 were used to calculate the formation constants of $[Hg(L)_m(H_2O)_n]^{2-mq}$ complexes for the three methods. We investigate $Hg^{2+}$ complexes with the same set of ligands that we studied in ref 35.

## 4. RESULTS AND DISCUSSION

As discussed previously, the solvation free energy of $[Hg(H_2O)_6]^{2+}$ can be calculated by using either the monomer cycle, Scheme 1 and eq 1, or the cluster cycle, Scheme 2 and eq 4. These two different methods will have an effect on the computation of the formation constants for $Hg^{2+}$ complexes. We will, first, discuss the formation of water clusters, which is the only difference between the monomer and cluster cycles, Schemes 1 and 2, using various radii (Bondi, Pauling, UA0, UAHF, UAKS, and UFF). Second, we discuss the solvation free energy of $[Hg(H_2O)_6]^{2+}$ as mentioned above in this paragraph. Finally, we discuss and calculate the solvation free energies and the formation constants of Hg(II) complexes.

**4.1. Solvation of Water and Water Clusters.** According to previous experimental and theoretical studies, water clusters can have a variety of different structures.[76−83] Some of the theoretical structures are global minima on their potential energy surface; others are local minima or transition states. The structures of $(H_2O)_n$, $n$ = 1−10, that are given in Figures 1 and SM1 (Supporting Information) can be classified into three sets, open chain (structures 1−3), cyclic (structures 4−7), and bridge (structures 8−11), Figure 1. Each set has different structures depending on the orientation and donation or accepting nature of the hydrogen atoms (hydrogen bonds). Moreover, the clusters might have overall symmetry, e.g., $C_i$ (structure 15), $D_{2d}$ (structure 39), and $S_4$ (structures 5 and 9), Figures 1 and SM1 (Supporting Information). In this section, we will evaluate the computational protocol and the accuracy of different cavity radii from the comparison between the calculated and experimental dipole moments and calculate the residual errors of the solvation free energy values, respectively.

The choice of the computational method (procedure) is an important point. The nature and connectivity of the hydrogen bonds are essential for the cluster structures (Figures 1 and SM1, Supporting Information). The dipole moment values, in the gas and aqueous phases, were used in comparison with the available experimental values as an indicator on the performance of radii type and level of theory; see Tables 1 and 2. The dipole moment of an isolated water monomer is 1.86 D,[78] whereas the corresponding value in the condensed phase increases to between 2.4 and 2.6 D as a result of polarization by the environment.[76] Theoretical studies of ice lattices have suggested even higher values of about 3.0 D.[79] A calculation using a coupled density functional/molecular mechanics Hamiltonian to simulate a quantum water molecule in a classical system gave a large fluctuation of the instantaneous value of the dipole moment of the quantum molecule.[83] Our


dx.doi.org/10.1021/jp5045089 | J. Phys. Chem. B 2014, 118, 11271−11283

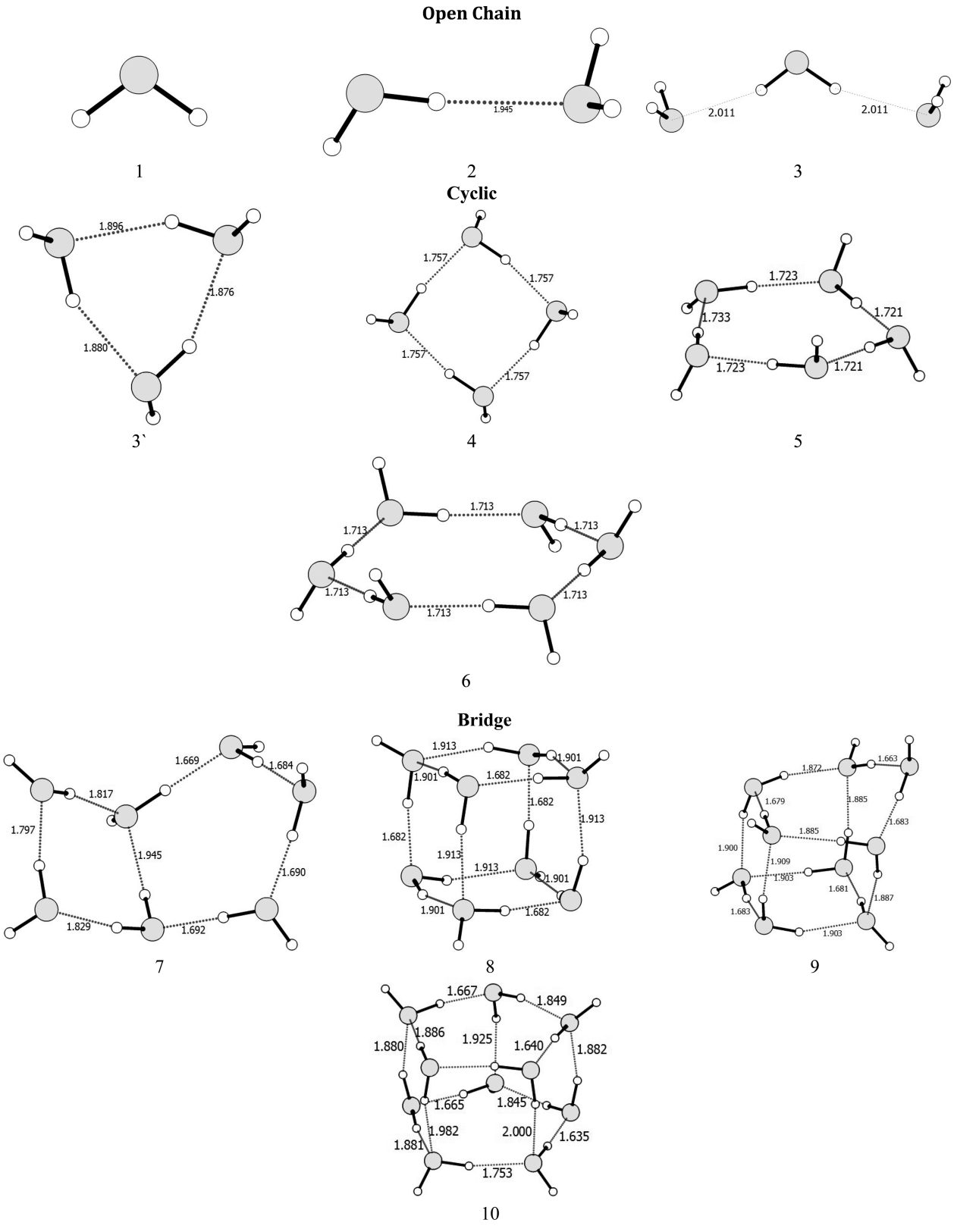


**Figure 1.** Optimized geometries of $(H_2O)_n$, $n$ = 1−10.

gas phase calculations give a dipole moment of 1.92 D for the isolated monomer, which is within 3% of the value observed experimentally (1.86 D), while the corresponding range in the condensed phase using different radii is 2.24−2.43 D. To calculate the total dipole moments of the water clusters, we considered only the most stable structures (Figure 1). The calculated dipole moment of the water dimer, 2.53 D, Table 1, is close to the experimental value of 2.64 D.[77] In general, we find that the B3LYP/cc-pVTZ level of theory can reproduce the dipole moments, and consequently the structures, of the water


dx.doi.org/10.1021/jp5045089 | J. Phys. Chem. B 2014, 118, 11271−11283

**Table 1. Absolute Aqueous Solvation Free Energies (kcal/mol) and Dipole Moments, $\mu$ (D), of the Most Stable Structure of $(H_2O)_n$ Clusters at $T$ = 298.15 K**

| cluster[a] | $\mu$[b] | $\Delta G^{\circ}_{g,bind}$ [c] | $\Delta G^{*}_{solv}$ [d] | $\Delta G^{*}_{solv}/n$ | overall stability[e] |
|---|---|---|---|---|---|
| 1 $H_2O$ | 1.92 | | | | |
| 2 $(H_2O)_2$ | 2.53 | 2.4 | −10.3 | −5.2 | −7.9 |
| 3 $(H_2O)_3$ | 1.25 | 2.7 | −12.5 | −4.2 | −9.8 |
| 4 $(H_2O)_4$ | 0.00 | 0.5 | −12.1 | −3.0 | −11.6 |
| 5 $(H_2O)_5$ | 1.11 | 0.5 | −14.1 | −2.8 | −13.6 |
| 6 (chair) $(H_2O)_6$ | 0.00 | 0.8 | −16.3 | −2.7 | −15.5 |
| 6 (cage) $(H_2O)_6$ | 2.13 | 3.1 | −18.6 | −3.1 | −15.5 |
| 6 (prism) $(H_2O)_6$ | 2.72 | 3.0 | −18.5 | −3.1 | −15.5 |
| 7 $(H_2O)_7$ | 3.97 | 1.5 | −18.9 | −2.7 | −17.4 |
| 8 $(H_2O)_8$ | 0.00 | −1.3 | −18.1 | −2.6 | −19.4 |
| 9 $(H_2O)_9$ | 1.64 | −1.2 | −20.2 | −2.9 | −21.4 |
| 10 $(H_2O)_{10}$ | 2.62 | −1.5 | −21.9 | −3.1 | −23.4 |

[a]The structures of $(H_2O)_n$, $n$ = 1−10, clusters are given in Figure 1. All the water clusters are global minima. [b]$\mu$: dipole moment in debye (D). [c]Calculated free energy of forming the water cluster in the gas phase. [d]Calculated by using the thermodynamic cycle shown (UAKS) in Scheme 3 and $\Delta G^{*}_{solv}(H_2O)$ = −6.32 kcal/mol. [e]Sum of $\Delta G^{\circ}_{g,bind}$ and $\Delta G^{*}_{solv}$.

clusters ($n$ = 1−10) similar to those published by Xantheas.[84] They are even closer to those obtained from high levels of theory, specifically MP2 with aug-cc-pVDZ[85] or aug-cc-pVTZ[86] basis sets and CCSD(T)[87] with TZ2P and aug-cc-pV5Z. Therefore, the popular B3LYP hybrid functional can be used along with the standard cc-pVTZ basis set. We will thus also apply this method to Hg(II) complexes to calculate the solvation free energies and formation constants at a reasonable cost. Complete information for the water clusters is given in Table TSM1 (Supporting Information).

The residual error has been calculated as the difference between the solvation free energy of the water cluster, $\Delta G^{*}_{solv}((H_2O)_n)$, calculated from the thermodynamic cycle in Scheme 3, and the direct output of G03, where one of the sources of error is the calculation of the binding energy in the gas phase (Table 2). In addition to the structure of the water cluster (as discussed above), another important factor when using a cluster/continuum approach with a cluster cycle is the selection of the radii of the implicit solvation model. The results shown in Table 2 indicate that the UFF radii fail to reproduce the $\Delta G^{*}_{solv}$ of the water clusters with $n$ > 3, as the calculated $\Delta G_{solv}$ values are positive. Also, the residual error increases almost linearly with the number of hydrogen bonds, Figure 2.

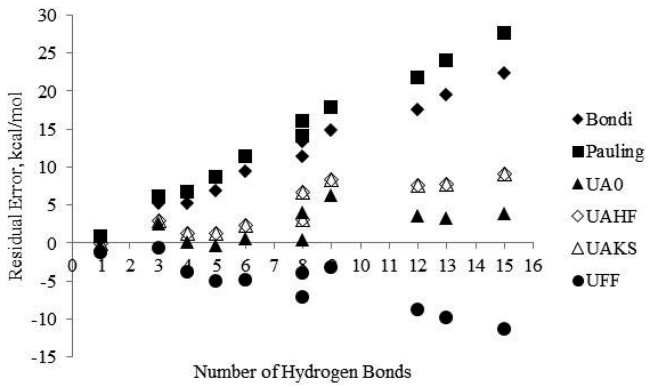


**Figure 2.** Correlation of the residual error for the cluster thermodynamic cycle depicted in Scheme 3 with the number of hydrogen bonds in the water cluster.

One of the main sources of these errors (Figure 2) is the failure of the continuum solvation methods to describe accurately the solvation of water clusters. On the other hand, the errors are considered negligible for $n \leq 6$ of the UA0, UAHF, and UAKS radii, Figure 2. The residual error ranges of UA0 and UAHF and UAKS for $n \leq 6$ are −0.4−2.6 and 0.02−3.1 kcal/mol, respectively, Table 2 and Figure 2. From the sign and magnitude of the residual error, one can conclude that using van der Waals radii such as the Bondi, Pauling, and UFF radii to create the cavity failed to reproduce the solvation free energy of the water clusters, while using the united atom topological model, in the form of UA0, UAHF, and UAKS, gives low residual errors. The residual errors of the $n$ = 6 water clusters (cage, prism, and chair structures) have been calculated by using the COSMO solvation model also. The average residual errors for the M06-L, M06-L-D3, B3LYP-D3, and CAM-B3LYP

**Table 2. Solvation Free Energies, Dipole Moments of Water Clusters, and the Total Residual Error of the Thermodynamic Cycle Shown in Scheme 3 Using the CPCM Continuum Solvation Model with Different Radii**

| | $\Delta G^{*}_{solv}$ [a] (kcal/mol) (dipole moment (D)) | | | | | residual errors[a] (kcal/mol) | | | | |
|---|---|---|---|---|---|---|---|---|---|---|
| cluster | Bondi | Pauling | UA0 | UAHF/UAKS | UFF | Bondi | Pauling | UA0 | UAHF/UAKS | UFF |
| $H_2O$ | −7.7 (2.40) | −8.3 (2.43) | −5.1 (2.28) | −5.6 (2.24) | −2.9 (2.24) | | | | | |
| $(H_2O)_2$ | −13.0 (2.86) | −14.2 (2.88) | −7.9 (2.79) | −8.8 (2.77) | −3.4 (2.79) | 0.5 | 0.8 | −0.4 | 0.0 | −1.3 |
| $(H_2O)_3$_c_uud | −16.6 (1.59) | −18.3 (1.60) | −9.0 (1.52) | −10.2 (1.50) | −2.1 (1.50) | 5.2 | 6.1 | 2.6 | 3.1 | −0.7 |
| $(H_2O)_4$_c_s4 | −17.6 (0.00) | −19.9 (0.00) | −7.4 (0.00) | −9.1 (0.00) | 1.7 (0.00) | 5.4 | 6.7 | 0.1 | 1.4 | −3.8 |
| $(H_2O)_5$_c2 | −20.9 (1.45) | −23.7 (1.46) | −8.2 (1.38) | −10.3 (1.36) | 3.2 (1.36) | 6.9 | 8.6 | −0.3 | 1.3 | −5.0 |
| $(H_2O)_6$_ch | −24.5 (0.00) | −27.8 (0.00) | −9.2 (0.00) | −11.8 (0.00) | 4.4 (0.00) | 9.5 | 11.4 | 0.6 | 2.4 | −5.0 |
| $(H_2O)_6$_cage | −26.8 (2.61) | −30.2 (2.63) | −11.6 (2.52) | −14.1 (2.50) | 2.1 (2.50) | 13.4 | 16.0 | 4.1 | 6.8 | −4.1 |
| $(H_2O)_6$_ps | −26.8 (3.33) | −30.1 (3.35) | −11.4 (3.23) | −14.0 (3.20) | 2.2 (3.20) | 15.0 | 17.8 | 6.3 | 8.5 | −3.3 |
| $(H_2O)_7$_ch2 | −28.5 (5.02) | −32.4 (5.06) | −10.7 (4.82) | −13.7 (4.75) | 5.2 (4.77) | 11.4 | 14.0 | 0.5 | 3.2 | −7.2 |
| $(H_2O)_8$_s4 | −29.1 (0.00) | −33.6 (0.00) | −8.7 (0.00) | −12.1 (0.00) | 9.5 (0.00) | 17.7 | 21.7 | 3.6 | 7.7 | −8.9 |
| $(H_2O)_9$_bg1 | −32.6 (2.09) | −37.6 (2.11) | −9.6 (2.03) | −13.5 (2.00) | 10.8 (1.99) | 19.6 | 24.0 | 3.4 | 7.9 | −9.9 |
| $(H_2O)_{10}$_cpcp1 | −35.6 (3.22) | −41.2 (3.23) | −10.1 (3.13) | −14.4 (3.10) | 12.6 (3.10) | 22.5 | 27.6 | 4.0 | 9.2 | −11.4 |
| absolute average | | | | | | 11.6 | 14.1 | 2.2 | 4.6 | 5.5 |

[a]Please see the text.


dx.doi.org/10.1021/jp5045089 | J. Phys. Chem. B 2014, 118, 11271−11283

Table 3. Solvation Free Energies (kcal/mol) of the $[Hg(H_2O)_6]^{2+}$ Complex (kcal/mol) as Calculated Using the Monomer Cycle and the Cluster Cycle with Three Different Structures of $(H_2O)_6$ Clusters

| | $\Delta G^*_{solv}$ | | | | | | | | | | |
|---|---|---|---|---|---|---|---|---|---|---|---|
| | B3LYP/CPCM (G03) | | | COSMO (NWChem) | | | | | | | |
| | UA0 | UAHF/UAKS[a] | estimated[b] | M06-L | estimated[b] | M06-L-D3 | estimated[b] | B3LYP-D3 | estimated[b] | CAM-B3LYP | estimated[b] |
| monomer | −277.8 | −169.6 | −173.0 | −208.8 | −195.0 | −208.0 | −194.2 | −179.3 | −165.5 | −184.8 | −171.0 |
| ch. cluster | −277.8 | | −172.2 | −207.3 | −166.7 | −206.5 | −181.9 | −177.8 | −169.9 | −183.3 | −175.3 |
| cg. cluster | −280.1 | | −169.8 | | −179.9 | | −180.9 | | −170.9 | | −173.9 |
| ps. cluster | −277.8 | | −169.9 | | −182.6 | | −184.9 | | −171.5 | | −174.2 |
| average | | | −171.2 | | −181.1 | | −185.5 | | −169.4 | | −173.6 |

[a]UAHF and UAKS give the same result for the $\Delta G^*_{solv}$ of $[Hg(H_2O)_6]^{2+}$, since they use the same H and O radii. [b]Estimated using eq 9 with $\Delta G^*_{solv,exptl}(Hg^{2+})$ = −420.6 kcal/mol.

Table 4. Solvation Free Energy (kcal/mol) and Formation Constants (log $K$) of $Hg(L)_m(H_2O)_n$ Using Different Methods, UAKS Radii, Monomer, and the Cluster Thermodynamic Cycle[a]

| | $\Delta G_{solv}$ | | | | log $K$ | | | |
|---|---|---|---|---|---|---|---|---|
| species | UAKS | monomer | cluster | ref[b] | UAKS | monomer | cluster | exptl[c] |
| $[Hg(Cl)(H_2O)_5]^+$ | −57.6 | −29.6 | −28.7 | −27.3 | 19.8 | 7.8 | 7.2 | 7.3 |
| $[Hg(Cl)_2(H_2O)_4]^0$ | −7.1 | 19.9 | 19.4 | 23.7 | 26.3 | 15.1 | 13.8 | 14.0 |
| $[Hg(Cl)_3(H_2O)_3]^{1-}$ | −32.2 | −6.8 | −11.3 | −9.6 | 26.5 | 16.5 | 15.1 | 15.0 |
| $[Hg(Cl)_4(H_2O)_2]^{2-}$ | −140.9 | −113.7 | −124.7 | −123.9 | 28.6 | 17.3 | 15.7 | 15.6 |
| $[Hg(OH)(H_2O)_5]^+$ | −62.7 | −31.9 | −32.8 | −35.0 | 8.1 | −4.1 | −3.4 | −3.4 |
| $[Hg(OH)_2(H_2O)_4]^0$ | −14.1 | 10.0 | 10.6 | 7.0 | −0.3 | −7.5 | −6.3 | −6.2 |
| $[Hg(Cl)(OH)(H_2O)_4]^0$ | −8.8 | 14.5 | 14.5 | 15.7 | 11.9 | 5.3 | 5.3 | 4.3 |
| $[Hg(SH)(H_2O)_5]^+$ | −55.0 | −39.5 | −39.5 | | 23.6 | 22.6 | 22.6 | 22.3 |
| $[Hg(SH)_2(H_2O)_4]^0$ | −3.8 | −9.4 | −9.4 | | 25.1 | 39.6 | 39.6 | 40.4 |
| $[Hg(S)(H_2O)_5]^0$ | −13.6 | −29.4 | −23.2 | | 9.8 | 31.8 | 27.2 | 29.8 |
| $[Hg(S)_2(H_2O)_4]^{2-}$ | −157.3 | −176.7 | −172.9 | | 0.4 | 25.0 | 23.9 | 25.5 |
| $[Hg(S)(SH)(H_2O)_4]^{1-}$ | −41.3 | −49.3 | −49.3 | | 16.6 | 32.9 | 32.9 | 34.6 |

[a]Only species with $m + n = 6$ are shown in the table; an extended version of this table is provided in the Supporting Information (Table TSM3). [b]Estimated using eq 10 with $\Delta G^*_{solv,ref}([Hg(H_2O)_6]^{2+})$ = −171.23 kcal/mol; see the text. [c]References 47, 48, and 90.

methods are 19.6, 12.7, 4.7, and 2.8 kcal/mol, respectively, Table TSM2 (Supporting Information).

**4.2. Calculation of $\Delta G^*_{solv}([Hg(H_2O)_6]^{2+})$.** The combination of a cluster/continuum model with a water cluster (Scheme 2) provides an alternative approach to pure continuum solvation approaches for calculating the solvation free energy of ions. The underlying premise of this methodology is that the interactions between $[Hg(H_2O)_n]^{2+}$ and bulk water are similar to those between $(H_2O)_n$ and bulk water in the limit of large $n$.[28] It is therefore critical to ensure that calculations are well-converged w.r.t. the number of explicit water molecules. This could, on the other hand, significantly increase the computational cost due to the need to locate the low-energy isomers of relatively large solute−water clusters. Accordingly, one should work systematically to establish the minimum number of water molecules required to saturate the first shell of the $Hg^{2+}$ ion and the ligands as well.

A factor that must be taken into consideration is the hydration of the metal ion, $Hg^{2+}$, since transfer from the gas phase into aqueous medium involves a gain of hydration free energy. Since the calculated hydration energy values of $Hg^{2+}$, as bare ion, could be larger or lower than the experimental ones, this potential error must be overcome by the complexation with six water molecules (saturated first shell). Solvation free energies of $[Hg(H_2O)_6]^{2+}$ are calculated using thermodynamic cycles 1 (monomer) and 2 (cluster). The solvation free energies of $[Hg(H_2O)_6]^{2+}$ have been calculated using CPCM and the most reliable radii, UA0, UAHF, and UAKS (as established in the previous section), and using the COSMO model as implemented in NWChem. The chair (7), prism (28), and cage (29) structures of the water clusters have been used (Figures 1 and SM1, Supporting Information). Table 3 summarizes the calculated (from Schemes 1 and 2) and estimated "experimental" (eq 9) solvation free energy of $[Hg(H_2O)_6]^{2+}$, where $\Delta G^\circ_{g,bind}$ is calculated from the upper leg of the respective thermodynamic cycles.

$$\Delta G^*_{solv}([Hg(H_2O)_6]^{2+}) = \Delta G^*_{solv,exptl}(Hg^{2+}) - \Delta G^\circ_{g,bind} \quad (9)$$

The calculated values of $\Delta G^*_{solv}(Hg^{2+})$ using the UA0 and UAHF/UAKS radii are, respectively, −520.2 and −409.4 kcal/mol. The experimental solvation free energy value of the $Hg^{2+}$ ion is −420.6 kcal/mol. Thus, the best estimate of the solvation free energy of $Hg^{2+}$ is obtained with the UAHF and UAKS radii. On the other hand, the UA0 radius overestimates the $\Delta G^*_{solv}(Hg^{2+})$ by about 100 kcal/mol. The computations of $\Delta G^*_{solv}([Hg(H_2O)_6]^{2+})$ using the implicit/explicit solvation model with UAHF and UAKS radii yield solvation free energies that are within 0.3−3.0 kcal/mol from the estimated "experimental" (eq 9) solvation free energies, using different water structures (monomer and clusters), of hexahydrated $Hg^{2+}$, Table 3. M06-L/ and M06-L-D3/COSMO overestimate the estimated $\Delta G^*_{solv}$ of $[Hg(H_2O)_6]^{2+}$ with respect to the B3LYP/CPCM level of theory by about 10−14 kcal/mol, Table


dx.doi.org/10.1021/jp5045089 | J. Phys. Chem. B 2014, 118, 11271−11283

3. The average estimated values of $\Delta G^*_{solv}([Hg(H_2O)_6]^{2+})$ at the M06-L and M06-L-D3 levels of theory are −181.1 and −185.5 kcal/mol, Table 3. The corresponding values at B3LYP-D3/COSMO and CAM-B3LYP/COSMO are −169.4 and −173.6 kcal/mol, respectively, Table 3, which are very close to the values obtained from B3LYP/CPCM/UAKS. The use of the monomer or cluster models leads to reproducible values for $\Delta G^*_{solv}([Hg(H_2O)_6]^{2+})$. From these results, we conclude that we do not need to include a second hydration shell when using cluster/continuum models to calculate the solvation free energy of transition metal ions such as $Hg^{2+}$ in aqueous solutions.

We note from Table 3 that the "estimated experimental" (eq 9) solvation free energy of $[Hg(H_2O)_6]^{2+}$ varies only by about 3−4 kcal/mol for the three different $(H_2O)_6$ clusters and the monomer method. Moreover, it is not entirely clear which cluster or clusters best represents the actual experimental situation. Hence, a possible approach for dealing with this situation is to use the average (B3LYP/CPCM/UAKS, −171.2; M06-L, −181.1; M06-L-D3, −185.5; B3LYP-D3, −169.4; CAM-B3LYP, −173.6 kcal/mol). These values will be used to calculate the solvation free energies of $Hg^{2+}$ complexes, $[Hg(L)_m(H_2O)_n]^{2-mq}$.

**4.3. The Calculation of $\Delta G^*_{solv}([Hg(L)_m(H_2O)_n]^{2-mq})$ and log *K*.** *4.3.1. $\Delta G^*_{solv}([Hg(L)_m(H_2O)_n]^{2-mq})$.* The problem in the $[Hg(L)_m(H_2O)_n]^{2-mq}$ system is to obtain highly accurate values of the solvation free energies of $Hg^{2+}$ complexes where the experimental values are unavailable. The $Hg^{2+}$ complexes can be classified as neutral, positive, monoanionic, and dianionic complexes. The solvation free energies of $[Hg(L)_m(H_2O)_n]^{2-mq}$ have been calculated through Scheme 4. We use either the solvation free energies of the water monomer or the cluster of water molecules in the reactants or products. The data in Table 4 indicate that the solvation free energies of all classes are negative using the UAKS radii, Figure 3. The monomer method gives in some cases positive and, in other cases, negative solvation free energies for the neutral complexes. For example, the $\Delta G_{solv}$ values of $[Hg(Cl)_2(H_2O)_4]^0$ and $[Hg(Cl)(OH)(H_2O)_6]^0$ are 19.9 and 37.3 kcal/mol, respectively, Table 4. The corresponding values of the same complexes without addition of water molecules are −24.2 and −16.7 kcal/mol, respectively, Table 4. The monomer method produces negative solvation free energy values for the charged $Hg^{2+}$ complexes except for $[Hg(OH)(H_2O)_9]^+$. On the other hand, the cluster method gives positive solvation free energies for neutral $Hg^{2+}$ complexes except for $[Hg(OH)_2]^0$, $[Hg(SH)_2(H_2O)_{4\text{ and }6}]^0$, and $[Hg(S)(H_2O)_{1,6,\text{ and }9}]^0$. It produces negative solvation free energies for all charged $Hg^{2+}$ complexes except for $[Hg(S)(SH)(H_2O)_6]^-$ (13.2 kcal/mol), Table 4 and Figure 3. As already mentioned, one of our goals is to accurately determine the solvation free energies of $Hg^{2+}$ complexes in solution that are unavailable experimentally. As a step toward this end, we calculated the $\Delta G^*_{solv}$ of $[Hg(Cl)_m(H_2O)_n]^{2-m}$, $[Hg(OH)_m(H_2O)_n]^{2-m}$, and $[Hg(Cl)(OH)(H_2O)_n]$ complexes where reliable experimental data is available. We will consider these solvation free energies as reference solvation free energies, $\Delta G^*_{solv,ref}$. The reference solvation free energies of $Hg^{2+}$ complexes can be calculated using the following equation

$$\Delta G^*_{solv,ref}([Hg(L)_m(H_2O)_n]^{2-mq}) \sim \Delta G^*_{solv,estimated}([Hg(H_2O)_6]^{2+}) - \Delta G^\circ_{g,bind} \pm m\Delta G^*_{solv,exptl}(L^q) \quad (10)$$

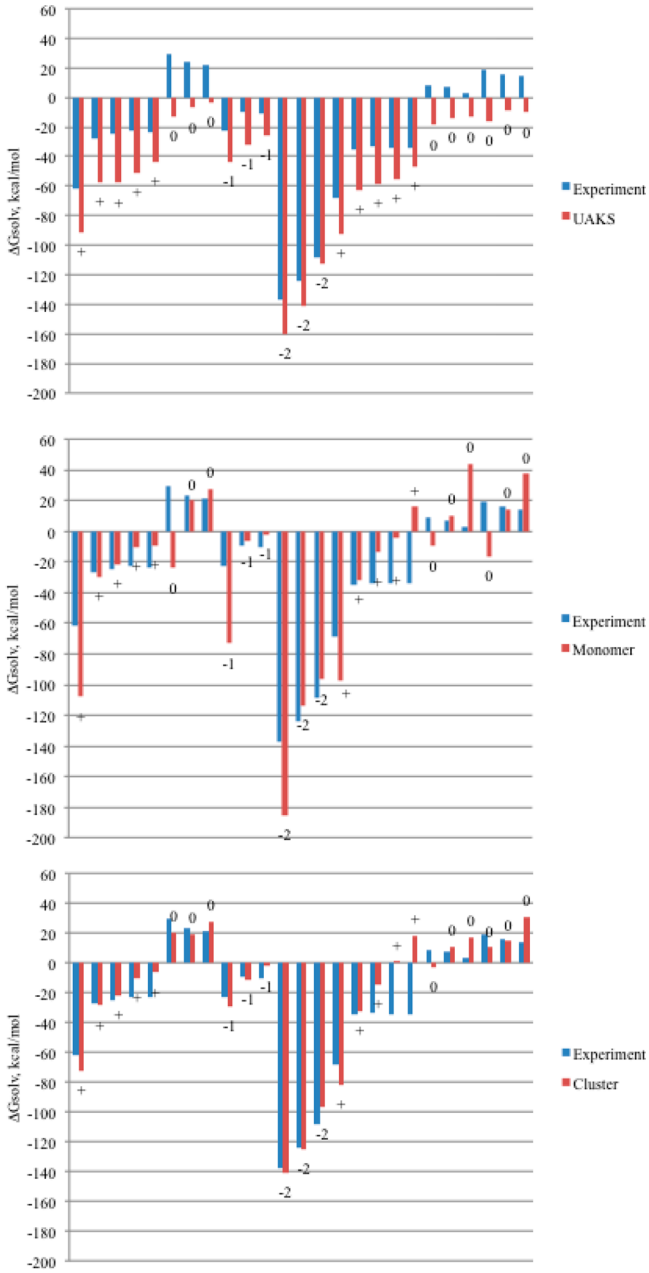


**Figure 3.** Deviation of the calculated solvation free energies from the estimated experimental solvation free energies (eq 10) for the first 25 complexes in Table 4. The charges of the complexes are given as well.

The sign of the last term depends on the ligand position. If the ligand is one of the reactants, we add the $\Delta G^*_{solv,exptl}(L^q)$; otherwise, if the ligand is only present in the $Hg^{2+}$ complex, we subtract the $\Delta G^*_{solv,exptl}(L^q)$. Put differently, if we added a ligand to form the $Hg^{2+}$ complex as shown in the following reaction

$$[Hg(H_2O)_6]^{2+} + mL^q \leftrightarrow [Hg(L)_m(H_2O)_n]^{2-mq}$$

we will add the $\Delta G^*_{solv}(L^q)$ in eq 10. However, if no ligand was added to form $Hg^{2+}$ complexes, like in

$$H_2O + [Hg(H_2O)_6]^{2+} \leftrightarrow [Hg(OH)_m(H_2O)_n]^{2-m} + mH_3O^+$$

we will subtract the $\Delta G^*_{solv}(L^q)$. The experimental solvation free energies of $[Hg(H_2O)_6]^{2+}$, $Cl^-$, $HS^-$, $HO^-$, and $H_2S$ are


dx.doi.org/10.1021/jp5045089 | J. Phys. Chem. B 2014, 118, 11271−11283

**Table 5. Formation Constants (log *K*) of $Hg(L)(H_2O)_5$ and $Hg(L)_2(H_2O)_4$ Using Different Methods, Different Levels of Theories (M06-L, M06-L-D3, B3LYP, B3LYP-D3, and CAM-B3LYP), CPCM/UAKS Radii, and the COSMO Solvation Model, Monomer, and the Cluster Thermodynamic Cycle**

| | log *K* | | | | | | | | | |
|---|---|---|---|---|---|---|---|---|---|---|
| | COSMO | | monomer | | | | Cluster | | | |
| | M06-L | B3LYP | M06-L | M06-L-D3 | B3LYP-D3 | CAM-B3LYP | M06-L | M06-L-D3 | B3LYP-D3 | CAM-B3LYP |
| $HgCl(H_2O)_5$ | 6.6 | 7.2 | 4.7 | 4.7 | 7.8 | 6.8 | 6.1 | 6.1 | 7.0 | 7.8 |
| $HgCl_2(H_2O)_4$ | 23.5 | 11.1 | 9.3 | 9.3 | 12.6 | 11.2 | 10.8 | 11.5 | 13.4 | 13.7 |
| $HgCl_3(H_2O)_3$ | 31.3 | 26.0 | 14.0 | 14.0 | 15.3 | 14.5 | 14.7 | 15.5 | 14.5 | 14.5 |
| $HgCl4(H_2O)_2$ | 39.4 | 34.6 | 18.7 | 12.3 | 16.4 | 16.4 | 18.7 | 17.2 | 15.7 | 15.7 |
| $Hg(OH)(H_2O)_5$ | −27.6 | −24.1 | −5.2 | −4.7 | −5.4 | −5.4 | −3.7 | −3.6 | −3.9 | −3.2 |
| $Hg(OH)_2(H_2O)_4$ | −45.1 | −40.7 | −10.4 | −9.3 | −5.1 | −10.7 | −8.2 | −7.3 | −6.3 | −8.5 |
| $Hg(Cl)(OH)(H_2O)_4$ | −9.9 | −9.9 | −0.5 | −0.5 | 6.6 | 6.2 | 0.2 | 1.2 | 4.4 | 5.3 |
| average absolute error | 18.2 | 14.6 (52.9)[a] | 3.2 | 2.9 | 1.2 (1.1)[b] | 1.9 | 2.0 | 1.5 | 0.3 (0.2)[c] | 0.7 |

[a]Average absolute error of B3LYP/CPCM(UAKS). [b]Average absolute error of the B3LYP/monomer thermodynamic cycle. [c]Average absolute error of the B3LYP/cluster thermodynamic cycle.

−171.2, −79,[88] −73.7,[14] −106.3,[14] and −0.7[89] kcal/mol, respectively. Thus, for example,

$$\Delta G^{*}_{solv,ref}([Hg(Cl)(H_2O)_5]^{+}) = -171.2 - (-222.8) + (-79.0) = -27.3 \text{ kcal/mol}$$

but

$$\Delta G^{*}_{solv,ref}([Hg(OH)_2(H_2O)_4]^{0}) = -171.2 - 34.3 - 2*(-106.3) = 7.1 \text{ kcal/mol}$$

(see Table 4).

Taking the best values of the calculated $\Delta G^{*}_{solv}$ of the different methods (UAKS radii, monomer, and cluster), we can evaluate these methods. We find that the UAKS radii overestimate the calculated $\Delta G^{*}_{solv}$ by about 17, 22, 14, and 4 kcal/mol (as average values), Figure 3, for cationic, neutral, monoanionic, and dianionic $Hg^{2+}$ complexes, respectively. Regarding the monomer approach, the corresponding values underestimate the calculated $\Delta G^{*}_{solv}$ by about 0.5, 1, 3, and 10 kcal/mol, respectively, with respect to the $\Delta G^{*}_{solv}$ values that were calculated using UAKS radii without using Scheme 4. This is also true for all complexes when using the cluster approach except for the neutral complexes. Results of similar magnitude, except for the last value, were obtained from the cluster method. The respective values are 0.5, 1, 2, and 1 kcal/mol, Figure 3. The data in Figure SM2 (Supporting Information) show a correlation between the calculated values of the experimental solvation free energy, using eq 10, and the calculated $\Delta G^{*}_{solv}$, using different methods (UAKS radii, monomer, and cluster and Scheme 4a). There is a significant improvement in the calculations of $\Delta G^{*}_{solv}$ in the cluster method, Figure SM2 (Supporting Information), with respect to the monomer method and UAKS radii. The goodness of fit, $R^2$, of UAKS, monomer, and cluster are 0.74, 0.90, and 0.97, respectively, Figure SM2 (Supporting Information). Consequently, we can conclude that the cluster method gives the best results.

The solvation free energies of the $[Hg(S)_m(H_2O)_n]^{2-2m}$, $[Hg(SH)_m(H_2O)_n]^{2-m}$, and $[Hg(S)(SH)(H_2O)_n]^{1-}$ were also calculated using UAKS radii, monomer, and cluster methods, Table 4. Generally speaking, all methods give negative solvation free energies for the above complexes. The only exception is the cluster method for $[Hg(SH)_2(H_2O)_6]^0$, $[Hg(S)(H_2O)_6]^0$, and $[Hg(S)(SH)(H_2O)_6]^-$. The corresponding values are 30.9, 31.7, and 13.2 kcal/mol, Table 4. However, the trend of decreasing solvation free energy values due to the addition of water molecules is the same for the three methods, Table 4.

*4.3.2. Formation Constants log K.* Shown in Tables 4 and 5 are the formation constants, log *K*, calculated using eq 8, as well as the experimental (for chloride and hydroxide complexes) and extrapolated (for sulfide and bisulfide complexes, Table 4) log *K* values for all $Hg^{2+}$ complexes studied in this work. For those formation constants calculated using eq 8, we used the experimental values for $\Delta G^{\circ\rightarrow *}(H_2O)$, $RT\ \ln[H_2O]$, $\Delta G_{vap}(H_2O)$, and $\Delta G^{*}_{solv}([Hg(H_2O)_6]^{2+})$ and the calculated values for the $\Delta G^{\circ}_{g,bind}$ and $\Delta G^{*}_{solv}((H_2O)_n)$. A plot of the experiment and the extrapolated log *K* against the calculated free energy of solution for the best results of UAKS radii, monomer, and cluster methods to calculate log *K* of $Hg^{2+}$ complexes yields goodness of fit values, $R^2$, of 0.89, 0.98, and 0.99, respectively, Figure 4. Table 4 also shows the effects of the addition of improper numbers of explicit water molecules on the calculated values of log *K*. For example, using the cluster method for $[Hg(Cl)(H_2O)_n]^+$ to calculate the log *K* by adding one water molecule or more than five water molecules will increase or decrease the solvation free energy of the complex and consequently decrease or increase the formation constant,

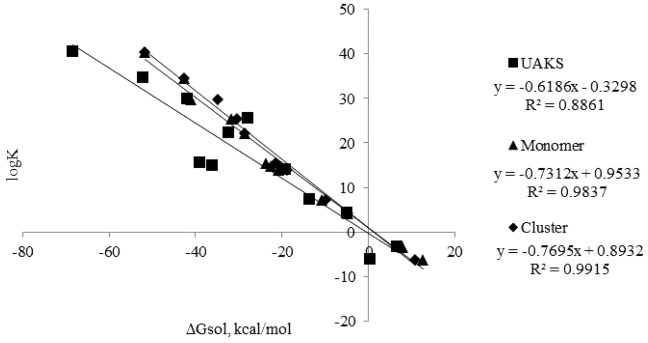


**Figure 4.** Experimental and extrapolated log *K* plotted against the calculated free energy of solution.


dx.doi.org/10.1021/jp5045089 | J. Phys. Chem. B 2014, 118, 11271−11283

log $K$. The corresponding values, respectively, are 9.7, 7.2, 0.0−11.3, and −17.7 for $n$ = 1, 5, 6, 7, and 9, Table 4. This can be compared to the experimental value of 7.3. Table 5 shows, for the most important structures of Hg(II) complexes, $Hg(L)(H_2O)_5$ and $Hg(L)_2(H_2O)_4$, the effect of the COSMO solvation model and the choice of functional (M06-L, M06-L-D3, B3LYP, B3LYP-D3, and CAM-B3LYP) on the calculated values of the formation constants, log $K$. For example, using the dispersion correction at the B3LYP level of theory (B3LYP-D3) and the COSMO solvation model decreases the average absolute error for the calculated log $K$ slightly. The corresponding values, using the monomer thermodynamic cycle with and without dispersion correction, are 1.2 and 1.1, respectively, Table 5. Furthermore, using the cluster models of the water molecules (cage, prism, and chair structures) modifies the calculated log $K$ values significantly, Table 5. The average absolute errors of COSMO/M06-L, monomer/M06-L, and cluster/M06-L are 18.2, 3.2, and 2.0, respectively, Table 5.

On the basis of the results presented here, we can draw several conclusions regarding the calculation of the formation constants, log $K$. First, the implicit solvent model, without being augmented with explicit water molecules, is unable to calculate the log $K$ for $[Hg(Cl)_m]^{2-m}$, $[Hg(OH)_m]^{2-m}$, and $[Hg(Cl)(OH)]$ (where reliable experimental data is available). Second, it is encouraging that a simple approach in which a complete first solvation shell of four (in the case of $m$ = 2) or five water molecules (for $m$ = 1) is added to the calculation increases the accuracy dramatically. Put differently, using atom-type radii with different water models (monomer and cluster) is much more straightforward than making large adjustments to the boundary between the solute and the continuum solvent (e.g., making large adjustments in the values used for the empirical atomic radii). Finally, applying the strategy outlined above yields a regression equation between the experimental log $K$ and the calculated formation constant that shows reasonably good correlation for the cluster model for complexes $[Hg(L)(L')(H_2O)_4]^0$, where L or L′ = $Cl^-$ or $HO^-$. The reason why adding explicit water might not always make the calculation more accurate is that the free energies of cavitation and dispersion and the solute's translational, vibrational, and rotational free energy all change upon solvation, and the parametrized surface tension and the explicit solute−water and (possible) water−water interactions are not necessarily accurate enough to account for these small changes quantitatively. As an example of how large errors can be reduced, we note that the log $K$ values calculated for $[Hg(Cl)(H_2O)]^+$ and $[Hg(OH)_2]$ are 9.7 and 17.5, respectively, using the cluster method. Completing the first solvation shell by adding four explicit water molecules to $[Hg(Cl)(H_2O)]^+$ and $[Hg(OH)_2]$ leads to calculated log $K$ values of 7.2 and −6.3, respectively, which are in excellent agreement with the experiment values of 7.3 and −6.2. We should also point out that, for $Hg^{2+}$ complexes with $Cl^-$ or $HO^-$, we obtain inferior results in most cases when we add more than four explicit water molecules. Following the same procedure for Hg(II) complexes with $S^{2-}$ and/or $HS^-$, we expect to obtain results that are of similar accuracy to those with $Cl^-$ and/or $HO^-$ ligands. Specifically, this procedure entails the following:

(1) Using theormodynamic cycles 1 and 4 to calculate $\Delta G^*_{solv}([Hg(H_2O)_6]^{2+})$ and $\Delta G^*_{solv}([Hg(L)_m(H_2O)_n]^{2-mq})$, respectively.
(2) Using appropriate water cluster models (six water molecules with three different cluster structures, chair conformer, prism, and cage, Figure 1).
(3) Choosing the best radii (UAKS/UAHF) according to the dipole moments and residual errors of the water clusters.
(4) The total number of the ligands ($S^{2-}$ and/or $HS^-$) and water molecules around the metal ion (Hg(II)-metal ion) should be sufficient to saturate the first shell.

For comparative purposes, with the reference solvation free energies of $Hg^{2+}$ complexes, we also calculated the log $K$ of $Hg^{2+}$ complexes using the thermodynamic cycle shown in Schemes 1 and 4 (i.e., no water cluster):

$$\Delta G^*_{solv}([Hg(L)_m(H_2O)_n]^{2-mq}) = \Delta G^*_{solv}([Hg(H_2O)_6]^{2+}) - m\Delta G^*_{solv}(L^q) - \Delta G^*_{bind} \pm n\Delta G_{vap}(H_2O) - x\Delta G^*_{solv}(H_3O^+) \quad (11)$$

Here $\Delta G^*_{solv}([Hg(H_2O)_6]^{2+})$ is equal to −171.2 kcal/mol as mentioned previously, $\Delta G^*_{solv}(L^q)$ and $\Delta G^*_{solv}(H_3O^+)$ are the aqueous solvation free energies of ligand $L^q$ and the hydronium ion ($H_3O^+$), respectively, and $x$ corresponds to the total absolute charge of the ligands $L_m$. The values used in eq 11 for $\Delta G^*_{solv}(L^q)$ were obtained from experiment, as mentioned in section 4.3.1. Calculating the above values and substituting into eq 11 leads to calculated log $K$ of $Hg^{2+}$ complexes using the monomer procedure, Tables 4 and 5.

For log $K$ calculations based on the water cluster model, we applied the thermodynamic cycle shown in Schemes 2 and 4, eq 12.

$$\Delta G^*_{solv}([Hg(L)_m(H_2O)_n]^{2-mq}) = \Delta G^*_{solv}([Hg(H_2O)_6]^{2+}) - m\Delta G^*_{solv}(L) - \Delta G^*_{bind} \pm RT\ln([H_2O]/n) \pm \Delta G^{\circ\to *} - \Delta G^*_{solv}((H_2O)_n) - x\Delta G^*_{solv}(H_3O^+) \quad (12)$$

Using this equation leads to calculated $\Delta G^*_{solv}([Hg(L)_m(H_2O)_n]^{2-mq})$ values of $Hg^{2+}$ complexes. These results are summarized in Tables 4 and 5, along with the results obtained using the CPCM/UAKS, COSMO, and monomer methods. For the cluster method, the data in Tables 4 and 5 are consistent with the statement above that adding explicit waters should almost always improve the results when the effect of the bulk solvent on the solvation free energy is large. Table 4 also shows that the accuracy of the log $K$ prediction decreases in a stepwise fashion as explicit waters are added beyond the completed first solvation shell. Finally, it is worth comparing results of the cluster method to those obtained using UAKS (or COSMO) and the monomer methods. This comparison clearly shows that using the cluster model of the water molecule improves the calculated values of the formation constants of $Hg^{2+}$ complexes.

## 5. CONCLUSIONS

Using DFT (B3LYP/cc-pVTZ//SDD(ECP) in combination with the conductor-like polarizable continuum model (CPCM) or an implicit/explicit hybrid solvation model for the calculation of the solvation free energies and the four thermodynamic cycles shown in Schemes 1−4, we have estimated the formation constant values, log $K$, for $Hg^{2+}$ complexes in aqueous solution. In many cases, when an accurate implicit solvent model is used, the addition of explicit


dx.doi.org/10.1021/jp5045089 | J. Phys. Chem. B 2014, 118, 11271−11283

solvent molecules is not necessarily required for obtaining reasonable estimates of the log $K$. However, when strong specific solute−solvent hydrogen bonding interactions are expected to play an important role in the aqueous phase (e.g., $[Hg(Cl)(OH)]$), adding four (or five, e.g., $HgCl^+$) explicit water molecules to the calculation significantly improves the accuracy of the log $K$ prediction.

The effect of the thermodynamic cycle and inclusion of explicit water molecules on the calculation of the formation constant, log $K$, values of $Hg^{2+}$ complexes has been investigated. Inclusion of explicit water molecules as monomers leads to more accurate log $K$ values than the continuum solvent model alone (UAKS radii). Inclusion of explicit water molecules as clusters results in further improvement. Therefore, the recommended procedure for calculating the log $K$ of $Hg^{2+}$ complexes with the CPCM or COSMO solvent models is to employ the cluster thermodynamic cycle and to include four or five water molecules, so as to get a completed first solvation shell on the aqueous species. It should be clarified that, even if nanoparticulate HgS(s) is present, our calculations still are valid if a proper thermodynamic cycle for the Hg(II) complexes can be established. In our thermodynamic cluster model (II), we obtain a larger log $K$ value for the formation of $[Hg(SH)(H_2O)_5]^+$ (0.3 log units larger in this model) and a smaller log $K$ for the formation of $[Hg(SH)_2(H_2O)_4]^0$, $[Hg(S)(H_2O)_5]^0$, $[Hg(S)_2(H_2O)_4]^{2-}$, and $[Hg(S)(SH)(H_2O)_4]^-$ (0.3, 0.8, 2.6, 1.6, and 1.7 log units smaller, respectively) compared to the original Benoit et al. model[47,48] (Table 4).

In summary, the following procedure is proposed. First, construct a suitable thermodynamic cycle (thermodynamic cycles 2, 3, and 4, cluster cycle) for the studied system. Second, use the water cluster models (chair, prism, and cage structures) and choose the best radii (UAKS or UAHF). Third, saturate the first shell of the species ($Hg^{2+}$) with water molecules, and then, estimate, using eq 9, the solvation free energy value, $\Delta G^*_{solv}([Hg(H_2O)_6]^{2+})$. Moreover, test the procedure with standard complexes like Hg(II) complexes with $Cl^-$ and/or $HO^-$.

We recommend that the following log $K$ (T = 25 °C, infinite dilution I = 0) are used in thermodynamic models describing the chemical speciation of Hg in the presence of sulfides:

$$[Hg(H_2O)_6]^{2+} + HS^- \Leftrightarrow [Hg(SH)(H_2O)_5]^+ + H_2O\text{: } 22.6$$

$$[Hg(H_2O)_6]^{2+} + 2HS^- \Leftrightarrow [Hg(SH)_2(H_2O)_4]^0 + 2H_2O\text{: } 39.6$$

$$[Hg(H_2O)_6]^{2+} + HS^- \Leftrightarrow [Hg(S)(H_2O)_5]^0 + H_3O^+\text{: } 27.2$$

$$[Hg(H_2O)_6]^{2+} + 2HS^- \Leftrightarrow [Hg(S)_2(H_2O)_4]^{2-} + 2H_3O^+\text{: } 23.9$$

$$[Hg(H_2O)_6]^{2+} + 2HS^- \Leftrightarrow [Hg(S)(SH)(H_2O)_4]^- + H_3O^+ + H_2O\text{: } 32.9$$

The above values are in good agreement with the extrapolated experimental values that are given in Table 4. Note that all of the species in these equations are aqueous molecules or ions where we have written the first solvation shell explicitly, in accordance with the procedure developed in this paper. To apply those reactions in chemical speciation models, for example, we could write the third reaction above as follows:

$$Hg^{2+}(aq) + HS^-(aq) \Leftrightarrow HgS^0(aq) + H^+(aq);\quad \log K = 27.2$$

(and similarly for the other reactions).

Finally, we note again that the uncertainty of the calculated log $K$ values for Hg(II) complexes with $Cl^-$ and/or $HO^-$ is generally within one unit. Thus, we believe that the accuracy for the molecules containing $S^{2-}$ and/or $HS^-$ will be in the same range of ±1 unit of log $K$.

## ■ ASSOCIATED CONTENT

### Supporting Information

Figures SM1 and SM2 showing global, local, and nonstable structures of water clusters and the relationship between the experimental solvation free energy values of the series of Hg(II) complexes with different models (UAKS, monomer, and cluster), respectively. Tables TSM1−TSM3 showing complete information for the water clusters, the total residual error of the thermodynamic cycle shown in Scheme 3, and an extended version of Table 4. This material is available free of charge via the Internet at http://pubs.acs.org.

## ■ AUTHOR INFORMATION

### Corresponding Author

*E-mail: schrecke@cc.umanitoba.ca.

### Notes

The authors declare no competing financial interest.

## ■ ACKNOWLEDGMENTS

G.S. and F.W. acknowledge funding from the Natural Sciences and Engineering Council of Canada (NSERC).

## ■ REFERENCES

(1) Cramer, C. J.; Truhlar, D. G. Implicit Solvation Models: Equilbiria, Structure, Spectra, and Dynamics. *Chem. Rev.* **1999**, *99*, 2161−2200.

(2) Orozco, M.; Luque, F. J. Theoretical Methods for the Description of the Solvent Effect in Biomolecular Systems. *Chem. Rev.* **2000**, *100*, 4187−4226.

(3) Tomasi, J.; Mennucci, B.; Cammi, R. Quantum mechanical continuum solvation models. *Chem. Rev.* **2005**, *105*, 2999−3093.

(4) Bennaim, A.; Marcus, Y. Solvation thermodynamics of nonionic solutes. *J. Chem. Phys.* **1984**, *81*, 2016−2027.

(5) Kelly, C. P.; Cramer, C. J.; Truhlar, D. G. Single-Ion Solvation Free Energies and the Normal Hydrogen Electrode Potential in Methanol, Acetonitrile, and Dimethyl Sulfoxide. *J. Phys. Chem. B* **2007**, *111*, 408−422.

(6) Marcus, Y. *Ion Solvation*; Wiley: Chichester, U.K., 1985.

(7) Andreussi, O.; Dabo, I.; Marzari, N. Revised self-consistent continuum solvation in electronic-structure calculations. *J. Chem. Phys.* **2012**, *136*, 064102.

(8) Chipman, D. M. C.; Chen, F. W. Cation electric field is related to hydration energy. *J. Chem. Phys.* **2006**, *124*, 144507.

(9) Chipman, D. M. Anion electric field is related to hydration energy. *J. Chem. Phys.* **2003**, *118*, 9937−9942.

(10) Camaioni, D. M.; Dupuis, M.; Bentley, J. Theoretical characterization of oxoanion, XOmn-, solvation. *J. Phys. Chem. A* **2003**, *107*, 5778−5788.

(11) Marenich, A. V.; Jerome, S. V.; Cramer, C. J.; Truhlar, D. G. Charge Model 5: An Extension of Hirshfeld Population Analysis for the Accurate Description of Molecular Interactions in Gaseous and Condensed Phases. *J. Chem. Theory Comput.* **2012**, *8*, 527−541.

(12) Zhang, S. M. A reliable and efficient first principles-based method for predicting $pK_a$ values. III. Adding explicit water molecules: can the theoretical slope be reproduced and pK(a) values predicted more accurately? *J. Comput. Chem.* **2012**, *33*, 517−526.

(13) Ribeiro, R. F.; Marenich, A. V.; Cramer, C. J.; Truhlar, D. G. Use of Solution-Phase Vibrational Frequencies in Continuum Models for the Free Energy of Solvation. *J. Phys. Chem. B* **2011**, *115*, 14556−14562.

(14) Kelly, C. P.; Cramer, C. J.; Truhlar, D. G. SM6: A density functional theory continuum solvation model for calculating aqueous solvation free energies of neutrals, ions, and solute-water clusters. *J. Chem. Theory Comput.* **2005**, *1*, 1133−1152.
(15) Kelly, C. P.; Cramer, C. J.; Truhlar, D. G. Aqueous solvation free energies of ions and ion-water clusters based on an accurate value for the absolute aqueous solvation free energy of the proton. *J. Phys. Chem. B* **2006**, *110*, 16066−16081.
(16) Kelly, C. P.; Cramer, C. J.; Truhlar, D. G. Adding explicit solvent molecules to continuum solvent calculations for the calculation of aqueous acid dissociation constants. *J. Phys. Chem. A* **2006**, *110*, 2493−2499.
(17) Pliego, J. R.; Riveros, J. M. The cluster-continuum model for the calculation of the solvation free energy of ionic species. *J. Phys. Chem. A* **2001**, *105*, 7241−7247.
(18) Pliego, J. R.; Riveros, J. M. Theoretical calculation of pK(a) using the cluster-continuum model. *J. Phys. Chem. A* **2002**, *106*, 7434−7439.
(19) Martin, R. L.; Hay, P. J.; Pratt, L. R. Hydrolysis of ferric ion in water and conformational equilibrium. *J. Phys. Chem. A* **1998**, *102*, 3565−3573.
(20) Asthagiri, D.; Pratt, L. R.; Ashbaugh, H. S. Absolute hydration free energies of ions, ion-water clusters, and quasichemical theory. *J. Chem. Phys.* **2003**, *119*, 2702−2708.
(21) Asthagiri, D.; Pratt, L. R.; Paulaitis, M. E.; Rempe, S. B. Hydration structure and free energy of biomolecularly specific aqueous dications, including $Zn^{2+}$ and first transition row metals. *J. Am. Chem. Soc.* **2004**, *126*, 1285−1289.
(22) Li, J.; Fisher, C. L.; Chen, J. L.; Bashford, D.; Noodleman, L. Calculation of redox potentials and pK(a) values of hydrated transition metal cations by a combined density functional and continuum dielectric theory. *Inorg. Chem.* **1996**, *35*, 4694−4702.
(23) Rode, B. M.; Schwenk, C. F.; Hofer, T. S.; Randolf, B. R. Coordination and ligand exchange dynamics of solvated metal ions. *Coord. Chem. Rev.* **2005**, *249*, 2993−3006.
(24) Uudsemaa, M.; Tamm, T. Density-functional theory calculations of aqueous redox potentials of fourth-period transition metals. *J. Phys. Chem. A* **2003**, *107*, 9997−10003.
(25) Uudsemaa, M.; Tamm, T. Calculation of hydration enthalpies of aqueous transition metal cations using two coordination shells and central ion substitution. *Chem. Phys. Lett.* **2004**, *400*, 54−58.
(26) Rotzinger, F. P. Mechanism of water exchange for the di- and trivalent metal hexaaqua ions of the first transition series. *J. Am. Chem. Soc.* **1997**, *119*, 5230−5238.
(27) Wiebke, J.; Moritz, A.; Cao, X.; Dolg, M. Approaching actinide(+III) hydration from first principles. *Phys. Chem. Chem. Phys.* **2007**, *9*, 459−465.
(28) De Abreu, H. A.; Guimaraes, L.; Duarte, H. A. Density-functional theory study of iron(III) hydrolysis in aqueous solution. *J. Phys. Chem. A* **2006**, *110*, 7713−7718.
(29) Zhan, C. G.; Dixon, D. A. Absolute hydration free energy of the proton from first-principles electronic structure calculations. *J. Phys. Chem. A* **2001**, *105*, 11534−11540.
(30) Zhan, C. G.; Dixon, D. A. First-principles determination of the absolute hydration free energy of the hydroxide ion. *J. Phys. Chem. A* **2002**, *106*, 9737−9744.
(31) Zhan, C. G.; Dixon, D. A. Hydration of the fluoride anion: Structures and absolute hydration free energy from first-principles electronic structure calculations. *J. Phys. Chem. A* **2004**, *108*, 2020−2029.
(32) Tawa, G. J.; Topol, I. A.; Burt, S. K.; Caldwell, R. A.; Rashin, A. A. Calculation of the aqueous solvation free energy of the proton. *J. Chem. Phys.* **1998**, *109*, 4852−4863.
(33) Mejias, J. A.; Lago, S. Calculation of the absolute hydration enthalpy and free energy of $H^+$ and $OH^-$. *J. Chem. Phys.* **2000**, *113*, 7306−7216.
(34) Gutowski, K. E.; Dixon, D. A. Predicting the energy of the water exchange reaction and free energy of solvation for the uranyl ion in aqueous solution. *J. Phys. Chem. A* **2006**, *110*, 8840−8856.
(35) Afaneh, A. T.; Schreckenbach, G.; Wang, F. Density functional study of substituted (-SH, -S, -OH, -Cl) hydrated ions of $Hg^{2+}$. *Theor. Chem. Acc.* **2012**, *131*, 1174−1190.
(36) Schreckenbach, G.; Shamov, G. A. Theoretical Actinide Molecular Science. *Acc. Chem. Res.* **2010**, *43*, 19−29.
(37) Shamov, G. A.; Schreckenbach, G. Density functional studies of actinyl aquo complexes studied using small-core effective core potentials and a scalar four-component relativistic method. *J. Phys. Chem. A* **2005**, *109*, 10961−10974. *Correction:* Shamov, G. A.; Schreckenbach, G. *J. Phys. Chem. A* **2006**, *110*, 12072.
(38) Cossi, M.; Barone, V.; Cammi, R.; Tomasi, J. Ab initio study of solvated molecules: A new implementation of the polarizable continuum model. *Chem. Phys. Lett.* **1996**, *255*, 327−335.
(39) Asaduzzaman, A. M.; Schreckenbach, G. Chalcogenophilicity of Mercury. *Inorg. Chem.* **2011**, *50*, 3791−3798.
(40) Asaduzzaman, A.; Schreckenbach, G. Degradation Mechanism of Methyl Mercury Selenoamino Acid Complexes: A Computational Study. *Inorg. Chem.* **2011**, *50*, 2366−2372.
(41) Fitzgerald, W. F.; Engstrom, D. R.; Mason, R. P.; Nater, E. A. The case for atmospheric mercury contamination in remote areas. *Environ. Sci. Technol.* **1998**, *32*, 1−7.
(42) Lamborg, C. H.; Fitzgerald, W. F.; Damman, A. W. H.; Benoit, J. M.; Balcom, P. H.; Engstrom, D. R. Modern and historic atmospheric mercury fluxes in both hemispheres: Global and regional mercury cycling implications. *Global Biogeochem. Cycles* **2002**, *16* (4), 51-1−51-11.
(43) Selin, N. E. Global Biogeochemical Cycling of Mercury: A Review. *Annu. Rev. Environ. Resour.* **2009**, *34*, 43−63.
(44) Wang, F. Y.; Tessier, A. Cadmium complexation with bisulfide. *Environ. Sci. Technol.* **1999**, *33*, 4270−4277.
(45) US Environmental Protection Agency (EPA) 1997, vol. *V*, EPA452/R.
(46) Benoit, J. M.; Gilmour, C. C.; Mason, R. P.; Heyes, A. Sulfide controls on mercury speciation and bioavailability to methylating bacteria in sediment pore waters (vol 33, pg 951, 1999). *Environ. Sci. Technol.* **1999**, *33*, 1780−1780.
(47) Benoit, J. M.; Gilmour, C. C.; Mason, R. P.; Heyes, A. Sulfide controls on mercury speciation and bioavailability to methylating bacteria in sediment pore waters. *Environ. Sci. Technol.* **1999**, *33*, 951−957.
(48) Benoit, J. M.; Gilmour, C. C.; Mason, R. P. T. The influence of sulfide on solid phase mercury bioavailability for methylation by pure cultures of Desulfobulbus propionicus (1pr3). *Environ. Sci. Technol.* **2001**, *35*, 127−132.
(49) Goulet, R. R.; Holmes, J.; Page, B.; Poissant, L.; Siciliano, S. D.; Lean, D. R. S.; Wang, F.; Amyot, M.; Tessier, A. Mercury transformations and fluxes in sediments of a riverine wetland. *Geochim. Cosmochim. Acta* **2007**, *71*, 3393−3406.
(50) Merritt, K. A.; Amirbahman, A. Mercury methylation dynamics in estuarine and coastal marine environments - A critical review. *Earth Sci. Rev.* **2009**, *96*, 54−66.
(51) Dyrssen, D.; Wedborg, M. The state of dissolved trace sulfide in seawater. *Mar. Chem.* **1989**, *26*, 289−293.
(52) Dyrssen, D.; Wedborg, M. The sulfur mercury (II) system in natural waters. *Water, Air, Soil Pollut.* **1991**, *56*, 507−519.
(53) Camaioni, D. M.; Schwerdtfeger, C. A. Comment on "Accurate experimental values for the free energies of hydration of $H^+$, $OH^-$, and $H_3O^+$". *J. Phys. Chem. A* **2005**, *109*, 10795−10797.
(54) Pliego, J. R. Thermodynamic cycles and the calculation of $pK_a$. *Chem. Phys. Lett.* **2003**, *367*, 145−149.
(55) Pliego, J. R. Reply to comment on: 'Thermodynamic cycles and the calculation of $pK_a$' [Chem. Phys. Lett. 367 (2003) 145]. *Chem. Phys. Lett.* **2003**, *381*, 246−247.
(56) Bryantsev, V. S.; Diallo, M. S.; Goddard, W. A. Calculation of solvation free energies of charged solutes using mixed cluster/continuum models. *J. Phys. Chem. B* **2008**, *112*, 9709−9719.
(57) Becke, A. D. Density-functional thermochemistry. 3. The role of exact exchange. *J. Chem. Phys.* **1993**, *98*, 5648−5652.

(58) Clark, T.; Chandrasekhar, J.; Spitznagel, G. W.; Schleyer, P. V. Efficient diffuse functio-augmented basis sets for anion calculations. III. The 3-21+G basis set or first-row elements, Li-F. *J. Comput. Chem.* **1983**, *4*, 294−301.
(59) Frisch, M. J.; Pople, J. A.; Binkley, J. S. Self-Consistent molecular-orbital methods. 25. Supplementary functions for Gaussian-basis sets. *J. Chem. Phys.* **1984**, *80*, 3265−3269.
(60) Krishnan, R.; Binkley, J. S.; Seeger, R.; Pople, J. A. Self-Consistent molecular-orbital methods. 20. Basis set for correlated wave-functions. *J. Chem. Phys.* **1980**, *72*, 650−654.
(61) Lee, C.; Yang, W.; Parr, R. G. Development of the Colle-Salvetti correlation energy formula into a functional of the electron density. *Phys. Rev. B* **1988**, *37*, 785−789.
(62) McLean, A. D.; Chandler, G. S. Contracted gaussian basis sets for molecular calculations. 1. 2nd row atoms, Z-11-18. *J. Chem. Phys.* **1980**, *72*, 5639−5648.
(63) Becke, A. D. Density functional exchange energy approximation with correct asymptitc behavior. *Phys. Rev. A* **1988**, *38*, 3098−3100.
(64) Li, J.; Zhu, T.; Hawkins, G. D.; Winget, P.; Liotard, D. A.; Cramer, C. J.; Truhlar, D. G. Extension of the platform of applicability of the SM5.42R universal solvation model. *Theor. Chem. Acc.* **1999**, *103*, 9−63.
(65) Cramer, C. J. *Essentials of Computational Chemistry Theories and Models*, 2nd ed.; John Wiley & Sons Ltd: Chichester, U.K., 2004.
(66) Barone, V.; Cossi, M. Quantum calculation of molecular energies and energy gradients in solution by a conductor solvent model. *J. Phys. Chem. A* **1998**, *102*, 1995−2001.
(67) Frisch, M. J.; Trucks, G. W.; Schlegel, H. B.; Scuseria, G. E.; Robb, M. A.; Cheeseman, J. R.; Montgomery, J. A., Jr.; Vreven, T.; Kudin, K. N.; Burant, J. C.; et al. *Gaussian 03*; Gaussian, Inc.: Wallingford, CT, 2003.
(68) Rappe, A. K.; Casewit, C. J.; Colwell, K. S.; Goddard, W. A., III; Skiff, W. M. UFF, a full periodic table force field for molecular mechanics and molecular dynamics simulations. *J. Am. Chem. Soc.* **1992**, *114*, 10024−10035.
(69) *Handbook of Chemistry and Physics*; Weast, R. C., Ed.; The Chemical Rubber Co.: Cleveland, OH, 1981.
(70) Bondi, A. Van der Waals Volumes + Radii. *J. Phys. Chem.* **1964**, *68*, 441−451.
(71) Valiev, M.; Bylaska, E. J.; Govind, N.; Kowalski, K.; Straatsma, T. P.; van Dam, H. J. J.; Wang, D.; Nieplocha, J.; Apra, E.; Windus, T. L.; de Jong, W. A. NWChem: A comprehensive and scalable open-source solution for large scale molecular simulations. *Comput. Phys. Commun.* **2010**, *181*, 1477−1489.
(72) Zhao, Y.; Truhlar, D. G. A new local density functional for main-group thermochemistry, transition metal bonding, thermochemical kinetics, and noncovalent interactions. *J. Chem. Phys.* **2006**, *125*, 194101.
(73) Yanai, T.; Tew, D. P.; Handy, N. C. A new hybrid exchange-correlation functional using the Coulomb-attenuating method (CAM-B3LYP). *Chem. Phys. Lett.* **2004**, *393*, 51−57.
(74) Klamt, A.; Schüürmann, G. COSMO - a new approach to dielectric screening in solvents with explicit expressions for the screening energy and its gradient. *J. Chem. Soc., Perkin Trans. 2* **1993**, 799−805.
(75) Grimme, S.; Antony, J.; Ehrlich, S.; Krieg, H. A consistent and accurate ab initio parametrization of density functional dispersion correction (DFT-D) for the 94 elements H-Pu. *J. Chem. Phys.* **2010**, *132*, 154104−154106.
(76) Coulson, C. A.; Eisenberg, D. Interactions of $H_2O$ molecules in ice. I. Dipole moment of an $H_2O$ molecule in ice. *Proc. R. Soc. London, Ser. A* **1966**, *291*, 445−453.
(77) Dyke, T. R.; Mack, K. M.; Muenter, J. S. Structure of water dimer from molecular beam electric resonance spectroscopy. *J. Chem. Phys.* **1977**, *66*, 498−510.
(78) Gregory, J. K.; Clary, D. C.; Liu, K.; Brown, M. G.; Saykally, R. J. The water dipole moment in water clusters. *Science* **1997**, *275*, 814−817.
(79) Heggie, M. I.; Latham, C. D.; Maynard, S. C. P.; Jones, R. Cooperative polarisation in ice I-h and the unusual strength of the hydrogen bond. *Chem. Phys. Lett.* **1996**, *249*, 485−490.
(80) Hendricks, J. H.; deClercq, H. L.; Lyapustina, S. A.; Bowen, K. H. Negative ion photoelectron spectroscopy of the ground state, dipole-bound dimeric anion, $(HF_2)^-$. *J. Chem. Phys.* **1997**, *107*, 2962−2967.
(81) Kim, K.; Jordan, K. D.; Zwier, T. S. Low- energy structures and vibrational frequencies of the water hexamer-compareson with benzene-$(H_2O)_6$. *J. Am. Chem. Soc.* **1994**, *116*, 11568−11569.
(82) Liu, K.; Brown, M. G.; Carter, C.; Saykally, R. J.; Gregory, J. K.; Clary, D. C. Characterization of a cage form of the water hexamer. *Nature* **1996**, *381*, 501−503.
(83) Tunon, I.; MartinsCosta, M. T. C.; Millot, C.; RuizLopez, M. F. A hybrid density functional classical molecular dynamics simulation of a water molecule in liquid water. *J. Mol. Model.* **1995**, *1*, 196−201.
(84) Xantheas, S. S. Ab-Initio studies of cyclic water clusters $(H_2O)_n$, n = 1−6. 3. Comparison of density functional with MP2 results. *J. Chem. Phys.* **1995**, *102*, 4505−4517.
(85) Odutola, J. A.; Dyke, T. R. Partially deutrated water dimers-microwave spectra and structure. *J. Chem. Phys.* **1980**, *72*, 5062−5070.
(86) Kemp, D. D.; Gordon, M. S. An interpretation of the enhancement of the water dipole moment due to the presence of other water molecules. *J. Phys. Chem. A* **2008**, *112*, 4885−4894.
(87) Klopper, W.; van Duijneveldt-van de Rijdt, J. G. C. M.; van Duijneveldt, F. B. Computational determination of equilibrium geometry and dissociation energy of the water dimer. *Phys. Chem. Chem. Phys.* **2000**, *2*, 2227−2234.
(88) Frese, K. W. Calculation of gibbs hydrtaded energy with the ion dielectric sphere model. *J. Phys. Chem.* **1989**, *93*, 5911−5916.
(89) Marenich, A. V.; Cramer, C. J.; Truhlar, D. G. Universal Solvation Model Based on Solute Electron Density and on a Continuum Model of the Solvent Defined by the Bulk Dielectric Constant and Atomic Surface Tensions. *J. Phys. Chem. B* **2009**, *113*, 6378−7396.
(90) Powell, K. J.; Brown, P. L.; Byrn, R. H.; Gajda, T.; Hefter, G.; Sjoberg, S.; Wanner, H. Chemical speciation of Hg(II) with environmental inorganic ligands. *Aust. J. Chem.* **2004**, *57*, 993−1000.
(91) Riccardi, D.; Guo, H. B.; Parks, J. M.; Gu, B. H.; Liang, L. Y.; Smith, J. C. Cluster-Continuum Calculations of Hydration Free Energies of Anions and Group 12 Divalent Cations. *J. Chem. Theory Comput.* **2013**, *9*, 555−569.
(92) Riccardi, D.; Guo, H. B.; Parks, J. M.; Gu, B. H.; Summers, A. O.; Miller, S. M.; Liang, L. Y.; Smith, J. C. Why Mercury Prefers Soft Ligands. *J. Phys. Chem. Lett.* **2013**, *4*, 2317−2322.

## NOTE ADDED IN PROOF

Recently, Riccardi et al.[91] computed the hydration free energies of the divalent group 12 metal cations $Zn^{2+}$, $Cd^{2+}$, and $Hg^{2+}$ (as well as $Cu^{2+}$) and the anions $OH^-$, $SH^-$, $Cl^-$ and $F^-$. Mixed cluster-continuum models were applied. Both the monomer and cluster cycles as well as the variational cluster continuum method were employed. Two different continuum solvation models were used to calculate the hydration free energies of the mercury ion, the SMD model and $PCM^{1.17}_{Bondi}$ for which the Bondi radii are scaled by a factor of 1.17. In a subsequent paper,[92] Riccardi et al. computed mercury ligand binding free energies for the same set of anionic ligands, plus $SeH^-$ and $Br^-$.